

# Towards Generalizable Reasoning: Group Causal Counterfactual Policy Optimization for LLM Reasoning

Jingyao Wang<sup>1 2 \*</sup> Peizheng Guo<sup>1 2 \*</sup> Wenwen Qiang<sup>1 2</sup> Jiahuan Zhou<sup>3</sup> Huijie Guo<sup>1 2</sup>  
Changwen Zheng<sup>1 2</sup> Hui Xiong<sup>4</sup>

## Abstract

Large language models (LLMs) excel at complex tasks with advances in reasoning capabilities. However, existing reward mechanisms remain tightly coupled to final correctness and pay little attention to the underlying reasoning process: trajectories with sound reasoning but wrong answers receive low credit, while lucky guesses with flawed logic may be highly rewarded, affecting reasoning generalization. From a causal perspective, we interpret multi-candidate reasoning for a fixed question as a family of counterfactual experiments with theoretical supports. Building on this, we propose **Group Causal Counterfactual Policy Optimization (GC<sup>2</sup>PO)** to explicitly train LLMs to learn generalizable reasoning patterns. It proposes an episodic causal counterfactual reward that jointly captures (i) robustness, encouraging the answer distribution induced by a reasoning step to remain stable under counterfactual perturbations; and (ii) effectiveness, enforcing sufficient variability so that the learned reasoning strategy can transfer across questions. We then construct token-level advantages from this reward and optimize the policy, encouraging LLMs to favor reasoning patterns that are process-valid and counterfactually robust. Extensive experiments on diverse benchmarks demonstrate its advantages.

## 1. Introduction

Large Language Models (LLMs) have evolved from handling basic natural language processing tasks to tackling complex reasoning problems (Jimenez et al., 2024; Zhou et al., 2025; Sadik & Govind, 2025). While pre-training establishes a foundation, realizing their full potential, particularly in specialized reasoning domains, requires targeted post-training adjustments (Tie et al., 2025). Consequently, Reinforcement Learning (RL) has emerged as a dominant paradigm to enhance reasoning capabilities (Shao et al., 2024; Zhang et al., 2024; Wang et al., 2025c). Among RL-based approaches, Group Relative Policy Optimization (GRPO) (Shao et al., 2024) and its variants (Zhang et al., 2025a; Gu et al., 2025; Wang et al., 2025b) have garnered significant attention by reducing computational overhead while delivering substantial performance gains.

Despite these advancements, a critical bottleneck remains: existing GRPO-based methods may struggle to achieve generalizable reasoning. The models frequently overfit to in-distribution benchmarks while failing to transfer skills to unseen questions, e.g., rephrasings, distractors, or harder variants (Figure 1). The root cause mainly lies in the misalignment of the reward signal. Specifically, current approaches primarily rely on outcome-based binary rewards (Shao et al., 2024; Yeo et al., 2025; Yang et al., 2025), assigning 1 to correct answers and 0 otherwise, regardless of the logical validity of the intermediate steps. Although some works use Process Reward Models (PRMs) (Wang et al., 2025b; Zhang et al., 2025b; Tan et al., 2025) to score intermediate steps, they are typically trained on chain-of-thought (CoT) traces filtered by final correctness, while abundant incorrect samples are treated as uniformly negative (Chen et al., 2025; Ye et al., 2025a). Thus, they may inherit the outcome bias: “lucky guesses” with flawed logic are incentivized, while rigorous reasoning processes that yield incorrect answers due to minor errors are blindly penalized. Our experiments further confirm this (Subsection 2.2): existing methods align more closely with final verification than intermediate soundness. This misalignment may encourage the LLMs to mimic answers rather than learn reasoning ideas, affecting the generalization of LLM reasoning.

\*Equal contribution <sup>1</sup>Institute of Software Chinese Academy of Sciences, Beijing, China <sup>2</sup>University of the Chinese Academy of Sciences, Beijing, China <sup>3</sup>Wangxuan Institute of Computer Technology, Peking University, Beijing, China <sup>4</sup>Thrust of Artificial Intelligence, The Hong Kong University of Science and Technology (Guangzhou), China. Department of Computer Science and Engineering, The Hong Kong University of Science and Technology Hong Kong SAR, China. Correspondence to: Wenwen Qiang <qiangwenwen@iscas.ac.cn>.

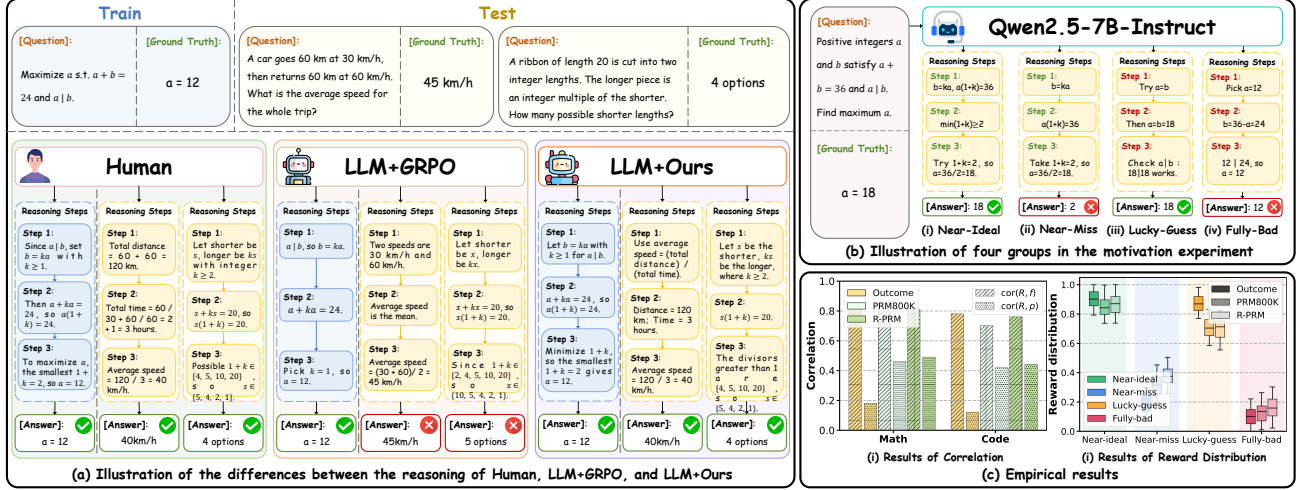


Figure 1. (a) Can LLMs “learn by analogy”: reasoning trajectories on representative questions. (b) Four trajectory groups defined by process validity and final correctness (Subsection 2.2). (c) Empirical results of the motivation experiment. See Appendix D.4 for details.

To address this challenge, we aim to answer a core question: how can we design fine-grained rewards for generalizable reasoning? From a causal perspective (Pearl, 2009), we argue that generalizable reasoning is fundamentally characterized by causal invariance: whether it captures stable mechanisms that transfer across variations, rather than by one-off correctness. As illustrated in Figure 2, generalizable reasoning relies on invariant structures (e.g., core constraints, correct variable binding, etc.) that hold true across different contexts, rather than spurious cues (e.g., seeing “average” and mechanically applying a fixed formula) that only correlate with success in a narrow distribution (Subsection 2.3). A model that learns invariant structures while filter out spurious cues can maintain performance even when questions change. Under the GRPO paradigm, the multiple trajectories generated for a single question can serve as counterfactual trials (Theorem 2.1). By analyzing how the reasoning process behaves across these parallel paths, we can identify patterns that are logically consistent, i.e., invariant structures that reveal generalizable reasoning patterns. Motivated by this, we propose two complementary principles for reward design: (i) robustness, which measures whether a reasoning pattern remains stable under local perturbations, indicating it has captured an invariant mechanism; and (ii) effectiveness, which ensures the reasoning step conveys sufficient task-relevant information, preventing the model from collapsing into trivial states. Unlike binary outcome labels, such a reward mechanism provides dense supervision, distinguishing between high-quality reasoning and lucky guesses even when the final answer is incorrect.

Based on the above analyses, we propose Group Causal Counterfactual Policy Optimization ( $GC^2PO$ ) for LLM reasoning. The core idea is proposing an episodic causal counterfactual reward that satisfies the above principles to explici-

tely evaluates the reasoning process. This reward consists of a stability term to measure causal invariance under perturbation and an expressiveness term to penalize uninformative representations using the optimal decay rate.  $GC^2PO$  operates in three integrated steps: (i) Episode segmentation (Subsection 3.1): we automatically break down solution paths into semantically complete reasoning steps; (ii) Reward design (Subsection 3.2): for each episode, we construct local perturbations in the representation space and calculate the causal counterfactual reward with a Monte Carlo estimator, jointly estimating robustness and effectiveness of the reasoning patterns; (iii) Policy optimization (Subsection 3.3): we combine episodic rewards with outcome rewards to allocate token-level advantages, encouraging the LLMs to prioritize generalizable reasoning patterns. Extensive experiments on various benchmarks demonstrate its advantages.

**The main contributions are as follows:** (i) We reveal a structural bias in existing GRPO-based post-training through empirical and causal analyses, demonstrating how current reward mechanisms entangle process validity with final correctness and hinder generalization. (ii) We propose  $GC^2PO$ , a novel framework that utilizes episodic causal counterfactual rewards to evaluate the robustness and effectiveness of underlying reasoning patterns. Building token-level advantages, it makes LLMs learn generalizable reasoning strategies. (iii) Across diverse benchmarks and models,  $GC^2PO$  consistently achieves superior performance.

## 2. Problem Settings and Analyses

### 2.1. Problem Settings

Our goal is to fine-tune a policy  $\pi_\theta$  (i.e., LLM) to answer arbitrary questions correctly. Taken GRPO (Shao et al., 2024) as an example: for each question  $x \sim \mathcal{D}$ , we sample

$K$  candidate trajectories  $\{y_k\}_{k=1}^K \sim \pi_{\theta_{\text{old}}}(\cdot|x)$  using the old policy  $\pi_{\theta_{\text{old}}}$ . For each  $y_k$ , we compute the outcome reward  $R_{\text{out}}(x, y_k) \in \{0, 1\}$  using an automatic verifier (e.g., correctness plus formatting), which equals 1 if  $y_k$  is correct. Next, we calculate a groupwise relative advantage:

$$A_k(x) = \frac{r_k - \bar{r}(x)}{\sqrt{s_r^2(x)}},$$

s.t.  $\bar{r}(x) = \frac{1}{K} \sum_{k=1}^K r_k$ ,  $s_r^2(x) = \frac{1}{K} \sum_{k=1}^K (r_k - \bar{r}(x))^2$ , (1)

By distributing this advantage uniformly over the tokens of  $y_k$ , we then optimize  $\pi_{\theta}$  by maximizing the following:

$$\begin{aligned} \mathcal{J}_{\text{GRPO}}(\theta) &= \mathbb{E}_{x \sim \mathcal{D}, \{y_k\} \sim \pi_{\theta_{\text{old}}}(\cdot|x)} \left[ \frac{1}{K} \sum_{k=1}^K \frac{1}{T_k} \sum_{t=1}^{T_k} \min \right. \\ &\quad \left. \left( \rho_{k,t}(\theta) A_k(x), \tilde{\rho}_{k,t}(\theta) A_k(x) \right) - \beta_{\text{KL}} \mu_{\text{KL}}(\pi_{\theta} \parallel \pi_{\text{ref}}) \right], \\ \text{s.t. } \rho_{k,t}(\theta) &= \frac{\pi_{\theta}(y_{k,t}|x, y_{k,< t})}{\pi_{\theta_{\text{old}}}(y_{k,t}|x, y_{k,< t})}, \quad \tilde{\rho}_{k,t}(\theta) = \text{clip}(\rho_{k,t}(\theta), 1 - \epsilon, 1 + \epsilon), \\ \mu_{\text{KL}}(\pi_{\theta} \parallel \pi_{\text{ref}}) &= \frac{\pi_{\text{ref}}(y_{k,t}|x, y_{k,< t})}{\pi_{\theta}(y_{k,t}|x, y_{k,< t})} - \log \frac{\pi_{\text{ref}}(y_{k,t}|x, y_{k,< t})}{\pi_{\theta}(y_{k,t}|x, y_{k,< t})} - 1, \end{aligned} \quad (2)$$

where  $\epsilon$  is the clipping radius,  $\beta_{\text{KL}}$  controls KL regularization  $\mu_{\text{KL}}$ , and  $\pi_{\text{ref}}$  is the reference policy.

## 2.2. Empirical Evidence

Despite strong performance, existing reward mechanisms are tightly coupled to final correctness rather than the reasoning process (Shao et al., 2024; Khalifa et al., 2025; Tan et al., 2025), affecting generalization. To validate this, we conduct an experiment for analysis.

Specifically, we construct an evaluation set from GSM8K (Cobbe et al., 2021), MATH (Hendrycks et al., 2021), and HumanEval (Chen et al., 2021), and use Qwen2.5-7B-Instruct to generate multiple trajectories per question. For each trajectory  $y_k$ , we record: (i) final correctness  $f_k \in \{0, 1\}$ , determined by symbolic solver or code execution; and (ii) process validity  $p_k \in [0, 1]$ , obtained from independent annotations of intermediate steps (human raters assisted by arithmetic checkers and code execution). We split the trajectories into four groups (Figure 1(b)) by evaluating whether their reasoning process and answer are correct, i.e., near ideal, near-miss, lucky guess, and fully bad. We then apply two families of reward mechanisms: (i) the outcome reward in GRPO (Shao et al., 2024); and (ii) representative PRMs, i.e., Qwen2.5-Math-7B-PRM800K and R-PRM-7B. We evaluate: (i) the correlation  $\text{cor}(R(\cdot), f)$  and  $\text{cor}(R(\cdot), p)$ ; and (ii) the rewards of different models over four groups. See Appendix G.1 for more details.

As shown in Figure 1(c), (i) existing methods align much more strongly with final correctness than with process validity:  $\text{cor}(R(\cdot), f)$  is much higher than  $\text{cor}(R(\cdot), p)$ ; (ii) the near-miss trajectories receive rewards close to fully bad trajectories, whereas lucky guesses obtain rewards comparable to truly high-quality solutions. These results underscore the

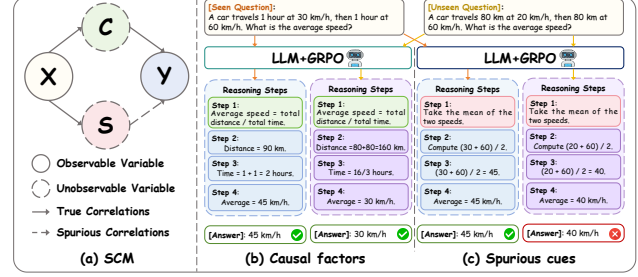


Figure 2. (a) SCM of LLM reasoning. (b) Examples of causal factors and spurious cues. See Appendix D.5 for more details.

limitations of existing reward mechanisms, which remain dominated by outcome signals and pay insufficient attention to the effectiveness and robustness of reasoning patterns.

## 2.3. Motivation Analysis

To address this limitation, in this subsection, we discuss the key question: how can we design fine-grained rewards that decouple process validity from final correctness, so as to encourage the LLMs to learn generalizable reasoning strategies rather than merely mimicking answers.

We adopt a causal perspective and conduct a Structural Causal Model (SCM) for analyses (Figure 2). Following (Pearl, 2009), we posit that for a given question  $x$ , the reasoning behavior of an LLM is jointly driven by two latent factors: (i) the causal factors  $c$ , which encodes task-governing mechanisms that remain valid under distribution shifts, e.g., arithmetic rules, logical consistency, and valid variable binding; and (ii) spurious cues  $s$ , which encapsulates brittle, dataset-specific shortcuts that coincide with correct answers only within a narrow context, e.g., reliance on specific formatting templates or shallow keyword associations. Achieving generalizable reasoning necessitates that the LLM relies on the invariant structure  $c$  rather than overfitting to the spurious correlations  $s$ . However, a challenge arises from the observational equivalence of existing reward mechanisms: a shortcut driven by  $s$  and a rigorous logical deduction driven by  $c$  yield the same correct final answer  $y$ ; the reward mechanisms that rely solely on verifying  $y$  cannot distinguish between the two, frequently assigning equal credit to both of them. It may encourage shortcut behavior through  $s \rightarrow y$ . To mitigate this, we aim to design a reward that assigns higher scores with  $c$  while filtering out  $s$ , encouraging the learning of generalizable reasoning.

To distinguish the causal factors  $c$  from spurious cues  $s$ , we propose to leverage the sampling mechanism inherent in GRPO to approximate a causal analysis. Instead of evaluating a single trajectory in isolation, we view the generation of multiple candidates as a set of counterfactual experiments. Formally, we establish the theoretical support as follows:

**Theorem 2.1.** *For a fixed input  $x$ , the reasoning of policy*

$\pi_\theta$  forms a Markov decision process (MDP) with transition kernel  $P(s_{t+1}|s_t, a_t)$ , satisfying: (i) There exists an SCM  $\mathcal{M}$ , without interventions, the trajectory distribution generated by  $\mathcal{M}$  coincides with that of the MDP. (ii) For any alternative policy  $\pi'_\theta$  or intervention on  $P(s_{t+1}|s_t, a_t)$ , the counterfactual trajectory distribution in  $\mathcal{M}$  coincides with the distribution obtained by simulating the modified MDP.

**Proof sketch.** This is a specialization of the main results in (Oberst & Sontag, 2019; Ness et al., 2019), which show that finite MDPs can be represented by SCMs where counterfactual distributions match the dynamics of the modified process. Under this perspective, for a question  $x$ , the sampled trajectories in GRPO can be viewed as parallel counterfactual experiments under shared exogenous noise but different reasoning paths. This perspective shifts the focus from identifying a single successful outcome to evaluating the structural stability of the reasoning process itself. By analyzing the variations across these parallel candidates, we can identify reasoning nodes that maintain logical consistency under perturbations, distinguishing them from those that are brittle or accidental. See Appendix B.1 for proofs.

Guided by this causal counterfactual perspective, we establish two core principles for our reward design: robustness and effectiveness. Robustness measures the stability of the answer distribution induced by a specific reasoning step when subjected to local perturbations. A high robustness score indicates that the step relies on an invariant logic  $c$  that persists across variations, rather than a brittle spurious cue. However, robustness alone is insufficient, as a trivial or empty state could also be highly stable. Therefore, we introduce effectiveness. It evaluates the information content of the step, ensuring that the reasoning conveys sufficient task-relevant information and does not collapse into trivial states. By integrating them, we move beyond binary outcome supervision. This design allows the LLMs to receive positive feedback for episodes that demonstrate sound reasoning logic, even if the final answer is incorrect; while penalizing trajectories that arrive at the correct answer through structurally flawed or spurious means, thereby enforcing the learning of generalizable reasoning.

### 3. Method

Based on these analyses, we propose Group Causal Counterfactual Policy Optimization (GC<sup>2</sup>PO). The core innovation is an episodic causal counterfactual reward. Instead of merely rewarding a trajectory that happens to be correct (which may rely on spurious shortcuts), our method evaluates whether the underlying reasoning pattern is truly generalizable. Specifically, GC<sup>2</sup>PO operates in three key steps. First, we automatically segment each question-solution pair into distinct episodes via prompt design (Subsection 3.1). Second, we compute a causal counterfactual reward for

each episode. This reward consists of two terms that jointly measure the robustness and effectiveness of the reasoning step (Subsection 3.2). Finally, for optimization, we leverage these rewards with the outcome reward to construct token-level advantages, optimizing the LLM to internalize generalizable reasoning strategies (Subsection 3.3). The framework is shown in Figure 3. The list of notations and pseudo-code are provided in Appendix A and Appendix C.

#### 3.1. Episode Segmentation

Reasoning tasks vary significantly in complexity. However, existing GRPO-based methods typically treat the entire solution as a single episode (Wiering & Van Otterlo, 2012; Szepesvári, 2022). This coarse granularity is insufficient for complex reasoning: it ignores the internal logical structure and fails to identify which specific step caused a success or failure. To enable fine-grained evaluation, we reformulate the reasoning process as a sequence of distinct episodes, where each episode represents a coherent logical step.

Formally, given a query  $x \sim \mathcal{D}$ , the sampling policy  $\pi_{\theta_{\text{old}}}$  generates a group of  $K$  candidate trajectories  $\{y_k\}_{k=1}^K$ . Each trajectory  $y_k$  consists of a reasoning chain  $z_k$  and a final answer  $a_k$ . We decompose the reasoning chain  $z_k$  into  $L_k$  discrete episodes, denoted as  $z_k = \{E_{k,l}\}_{l=1}^{L_k}$ , where each  $E_{k,l}$  corresponds to the tokens of the  $l$ -th reasoning step. In practice, we enforce this segmentation via prompt engineering. The model is instructed to delimit reasoning steps using specific tags (e.g., `<episode_i>` and `</episode_i>`, see Appendix G.5), ensuring that each  $E_{k,l}$  forms a self-contained semantic unit. This segmentation is crucial: it allows us to assign rewards to individual logical steps, enabling the model to learn from correct intermediate steps even if the final answer is incorrect.

#### 3.2. Reward Design

To determine whether an episode encodes a generalizable reasoning pattern, we propose an episodic causal counterfactual reward. The reward consists of: (i) a *stability term*: for robustness, it measures how much of the reasoning behavior of the episode survives under latent perturbations, and (ii) an *expressiveness term*: for effectiveness, it constrains the decay rate of the episode’s representation, ensuring that the reasoning step retains sufficient information to be effective across different contexts. By optimizing for both, the LLM is incentivized to converge toward reasoning patterns that are both robust and effective. In this subsection, we first clarify the roles of the two terms and then formally define the reward (Theorem 3.1). Next, we show how to compute it efficiently with theoretical guarantees (Theorem 3.2). Finally, we discuss why this reward is effective.

To simulate potential variations in the reasoning context, we operate within the continuous representation space. It

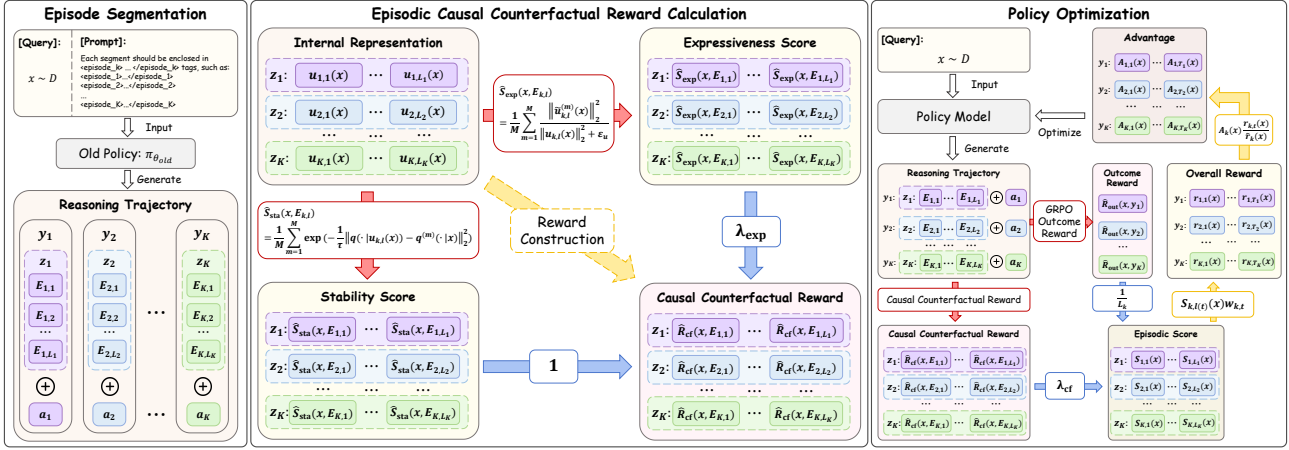


Figure 3. The framework of  $GC^2PO$ . It segments reasoning into episodes (Left), calculates episodic causal counterfactual reward via stability and expressiveness terms (Middle), and optimizes the policy by building token-level advantages (Right).

offers a more stable and computationally efficient alternative to perturbing discrete input tokens or model parameters (Wang et al., 2025b; 2024). For a given question  $x$  and episode  $E_{k,l}$ , we map the reasoning step to a latent vector  $u_{k,l}(x, E_{k,l}) \in \mathbb{R}^d$  (simplified write as  $u_{k,l}(x)$ ), which is derived from the hidden state of the last token. This vector determines the model’s answer distribution  $q(\cdot | u_{k,l}(x))$  over the answer space  $\mathcal{A}$ . We then apply a family of perturbation operators  $\{g_m\}_{m=1}^M$  to generate perturbed representations  $\tilde{u}_{k,l}^{(m)}(x) = g_m(u_{k,l}(x))$  and their induced answer distributions  $q(\cdot | \tilde{u}_{k,l}^{(m)}(x))$ . Intuitively,  $u_{k,l}(x)$  encodes “what this episode is trying to do”, while  $\tilde{u}_{k,l}^{(m)}(x)$  simulates nearby “what-if” scenarios. The stability term quantifies the divergence between  $q(\cdot | u_{k,l}(x))$  and  $q(\cdot | \tilde{u}_{k,l}^{(m)}(x))$ : episodes whose logic truly works under variations keep  $q(\cdot | u_{k,l}(x))$  and  $q(\cdot | \tilde{u}_{k,l}^{(m)}(x))$  close and thus receive high scores; brittle episodes exhibit large shifts and are penalized. The *expressiveness term* is defined from the viewpoint of the optimal decay rate (Cazenave & Haraux, 1998; Pazy, 2012): it tracks how fast the representation  $u_{k,l}(x)$  decays along perturbation directions. If the perturbations quickly drive  $u_{k,l}(x)$  toward a low-norm, uninformative state, the episode is structurally fragile and gets a low score; if the representation remains strong and decays slowly, the episode is rewarded. Together, they encourage episode representations that are both stable in their predictions and persistent in representation space. More analyses are provided in Appendix D.3.

We then present the formal definition of the episodic causal counterfactual reward with causal identifiability guarantees:

**Theorem 3.1.** For a fixed question  $x$  and episode  $E_{k,l}$ , let  $u_{k,l}(x) \in \mathbb{R}^d$  denote the episode representation and  $q(\cdot | u_{k,l}(x)) \in \Delta(\mathcal{A})$  the induced answer distribution. Let  $\{g_m\}_{m=1}^M$  be a family of perturbation operators acting on representations, and define  $\tilde{u}_{k,l}^{(m)}(x) = g_m(u_{k,l}(x))$  and

$q^{(m)}(\cdot | x) = q(\cdot | \tilde{u}_{k,l}^{(m)}(x))$ . Let  $\pi_\theta^*$  be any policy that achieves the highest causal counterfactual reward  $R_{cf}^*(x, E_{k,l})$ :

$$\begin{aligned} R_{cf}^*(x, E_{k,l}) &= S_{sta}(x, E_{k,l}) + \lambda_{exp} S_{exp}(x, E_{k,l}), \\ \text{s.t. } S_{sta}(x, E_{k,l}) &= \mathbb{E}_m \left[ \exp \left( -\frac{1}{\tau} \|q(\cdot | u_{k,l}(x)) - q^{(m)}(\cdot | x)\|_2^2 \right) \right], \\ S_{exp}(x, E_{k,l}) &= \mathbb{E}_m \left[ \frac{\|\tilde{u}_{k,l}^{(m)}(x)\|_2^2}{\|u_{k,l}(x)\|_2^2 + \varepsilon_u} \right], \end{aligned} \quad (3)$$

where  $\lambda_{exp}$  is weighting coefficient,  $\tau$  and  $\varepsilon_u$  are hyperparameters following (Pazy, 2012). Then,  $\pi_\theta^*$  block-identifies the true causal variables in the sense of Definition B.3.

**Proof sketch.** The proof relies on two main arguments. First, maximizing  $S_{sta}$  enforces invariance. Using the Darmois construction, we show that the representation mapping becomes independent of spurious cues, aligning solely with causal factors. Second, by analyzing the consistency of the induced answer distribution  $q(\cdot | u_{k,l}(x))$  under perturbation operators  $\{g_m\}_{m=1}^M$ , we show that the representation mapping (from the episode space to  $\mathbb{R}^d$ ) depends solely on causal blocks in a measure-theoretic sense, decoupling causal factors. Then, maximizing  $S_{exp}(x, E_{k,l})$  rules out degenerate solutions via an energy-preservation argument and yields a non-collapsed, maximum-entropy representation. By the inverse mapping theorem (Zimmermann et al., 2021; Dontchev & Hager, 1994), this implies an invertible correspondence between  $u_{k,l}(x)$  and  $c$ , establishing block-identification. See Appendix B.2 for full details.

**Intuition and Discussion.** A larger  $R_{cf}^*$  indicates a more valuable episode for optimization.  $S_{sta}(x, E_{k,l})$  is maximized when  $q(\cdot | u_{k,l}(x)) = q^{(m)}(\cdot | x)$  for all  $m$ , and decays exponentially as these distributions diverge; it therefore measures distributional robustness under perturbations.  $S_{exp}(x, E_{k,l})$  captures how well the representation avoids collapsing under perturbations: with a local linearization

$\tilde{u}_{k,l}^{(m)}(x) \approx A_m u_{k,l}(x)$ , the ratio estimates the squared gain of  $A_m$  along  $u_{k,l}(x)$ , and its expectation reflects the effective energy decay. Larger  $S_{\text{exp}}$  thus implies weaker decay and more informative representations. Thus,  $R_{\text{cf}}^*(x, E_{k,l})$  is large only when the episode is both stable and expressive.

Obtaining **Theorem 3.1**, we illustrate how to calculate it in practice. For each  $x$ , we run a forward pass to obtain  $u_{k,l}(x)$  and  $q(\cdot|u_{k,l}(x))$  with **Subsection 3.1**, then sample  $M$  perturbed representations  $\tilde{u}_{k,l}^{(m)}(x)$ . The implementation of the latent-space perturbation operators  $\{g_m\}_{m=1}^M$  are provided in **Appendix F**. Next, we compute the answer distributions  $q^{(m)}(\cdot|x)$  and norms, and substitute them into Eq.3 for  $S_{\text{sta}}$  and  $S_{\text{exp}}$ . Since computing  $S_{\text{sta}}(x, E_{k,l})$  and  $S_{\text{exp}}(x, E_{k,l})$  requires expectations over the full perturbation distribution, which are intractable in closed form, we approximate them with Monte Carlo estimators on  $M$  samples, expressed as:

$$\begin{aligned} \hat{R}_{\text{cf}}(x, E_{k,l}) &= \hat{S}_{\text{sta}}(x, E_{k,l}) + \lambda_{\text{exp}} \hat{S}_{\text{exp}}(x, E_{k,l}), \\ \text{s.t. } \hat{S}_{\text{sta}}(x, E_{k,l}) &= \frac{1}{M} \sum_{m=1}^M \exp \left( -\frac{1}{\tau} \|q(\cdot|u_{k,l}(x)) - q^{(m)}(\cdot|x)\|_2^2 \right), \\ \hat{S}_{\text{exp}}(x, E_{k,l}) &= \frac{1}{M} \sum_{m=1}^M \frac{\|\tilde{u}_{k,l}^{(m)}(x)\|_2^2}{\|u_{k,l}(x)\|_2^2 + \varepsilon_u}, \end{aligned} \quad (4)$$

Below, we establish the performance guarantee:

**Theorem 3.2.** *Let the latent manifold be  $\mathcal{Z} = \mathcal{C} \times \mathcal{S}$  endowed with a Riemannian metric, assume the perturbations  $\{g_m\}_{m=1}^M$  locally span the tangent space of the non-causal manifold  $T_s \mathcal{S}$  with **Assumption B.6**. If a learned  $u^*$  satisfies  $S_{\text{sta}} \geq 1 - \epsilon$  and  $S_{\text{exp}} \geq \gamma$ , then, maximizing  $R_{\text{cf}}^*$  minimizes the error bound to the oracle policy  $\pi_{\text{opt}}(\cdot|c) := \mathbb{E}_s[\pi^*(\cdot|c, s)]$  with  $\mathbb{E}_s[D_{\text{KL}}(\pi_{\text{opt}}(\cdot|c) \| \pi^*(\cdot|c, s))] \leq \mathcal{O}(\sqrt{\epsilon})$ .*

This theorem establishes that maximizing the proposed reward guarantees convergence to the optimal causal policy, i.e., the policy that leverages causal factors for reasoning.

**Proof sketch.** First, applying a first-order Taylor expansion to  $S_{\text{sta}}$  demonstrates that maximizing it suppresses the sensitivity to non-causal perturbations, yielding the bound  $\|\nabla_s \pi^*\|_F^2 \leq \mathcal{O}(\epsilon)$ . Second, regarding  $S_{\text{exp}}$  as a Rayleigh quotient, the Courant-Fischer theorem (Avron, 2008) implies that maximizing expressiveness guarantees a strictly positive singular value for the Jacobian along the causal manifold  $\mathcal{C}$ , thereby preventing representation collapse. Combining the suppressed non-causal sensitivity with the preserved causal structure directly bounds the KL divergence between the learned and oracle policies by  $\mathcal{O}(\sqrt{\epsilon})$ . See **Appendix B.3** for proofs and **Appendix B.4** for efficiency analysis.

Finally, we explain why the reward is effective. It operates at the episode level and evaluates how the encoded reasoning generalizes, rather than only final correctness. The episodes containing genuinely valid reasoning steps tend to induce answer distributions that remain stable un-

der mechanism-preserving perturbations, yielding high stability scores  $S_{\text{sta}}(x, E_{k,l})$ ; while their representations do not collapse or rapidly decay along perturbation directions, leading to large expressiveness scores  $S_{\text{exp}}(x, E_{k,l})$ . In contrast, brittle shortcuts or filler steps produce large distribution shifts or rapid representation decay, leading to low  $R_{\text{cf}}(x, E_{k,l})$  even when the final answer is accidentally correct. Thus, the reward provides a fine-grained signal that separates process validity from outcome correctness and steers the model toward robust, reusable reasoning patterns.

### 3.3. Policy Optimization

In this subsection, we illustrate the policy optimization of  $\text{GC}^2\text{PO}$ . Specifically, we integrate the proposed causal counterfactual reward with the outcome reward in a GRPO-style objective, considering both reasoning effectiveness and answer correctness. For each candidate  $y_k$  and episode index  $l$ , we define an episodic score that combines both rewards:

$$S_{k,l}(x) = \frac{1}{L_k} R_{\text{out}}(x, y_k) + \lambda_{\text{cf}} R_{\text{cf}}(x, E_{k,l}), \quad (5)$$

where  $\lambda_{\text{cf}}$  is a hyperparameter and  $R_{\text{out}}(x, y_k) \in \{0, 1\}$  is the outcome reward that is evenly distributed across episodes.

We then distribute episodic scores to tokens. For the  $t$ -th token of trajectory  $k$ , let  $l$  be the episode index such that  $y_{k,t} \in E_{k,l}$ . We define an unnormalized surprise weight under the old policy, i.e.,  $\tilde{w}_{k,t}(x) = -\log \pi_{\theta_{\text{old}}}(y_{k,t} | x, y_{k,t})$ , and normalize it as  $w_{k,t}(x)$ . The reward is then obtained:

$$\begin{aligned} r_{k,t}(x) &= S_{k,l(t)}(x) w_{k,t}(x), \\ \text{s.t. } w_{k,t}(x) &= \frac{\tilde{w}_{k,t}(x)}{\sum_{t' \in E_{k,l(t)}} \tilde{w}_{k,t'}(x)}. \end{aligned} \quad (6)$$

For each trajectory  $k$ , we aggregate the token-level rewards into a single scalar by taking a truncated mean over tokens (i.e., discarding a small fraction of extreme values), denoted by  $\tilde{r}_k(x) = \text{TruncMean}(\{r_{k,t}(x)\}_{t=1}^{T_k})$ . Across the  $K$  candidates for the same  $x$ , we compute the group-normalized advantage  $\hat{A}_k(x)$  with group-wise mean  $\bar{r}(x)$  and variance  $s_r^2(x)$  of these trajectory-level scores. We rescale this trajectory-level advantage back to tokens according to their relative contribution, obtaining  $A_{k,t}(x)$  with:

$$\begin{aligned} A_{k,t}(x) &= \hat{A}_k(x) \frac{r_{k,t}(x)}{\tilde{r}_k(x)}, \quad \text{s.t. } \hat{A}_k(x) = \frac{\tilde{r}_k(x) - \bar{r}(x)}{\sqrt{s_r^2(x)}}, \\ \bar{r}(x) &= \frac{1}{K} \sum_{k=1}^K \tilde{r}_k(x), \quad s_r^2(x) = \frac{1}{K} \sum_{k=1}^K (\tilde{r}_k(x) - \bar{r}(x))^2. \end{aligned} \quad (7)$$

In this way, even trajectories with  $R_{\text{out}}(x, y_k) = 0$  can receive positive advantages on episodes with high counterfactual rewards, converting previously negative groupwise advantages into useful learning signals for genuinely good but unlucky reasoning. Conversely, for trajectories with  $R_{\text{out}}(x, y_k) = 1$ , useless episodes obtain relatively small or even negative advantages after normalization, discouraging the model from reinforcing unstable reasoning patterns.

$GC^2PO$  then adopts a GRPO-style optimization objective at the token level based on the above advantages:

$$\begin{aligned} \mathcal{J}_{GC^2PO}(\theta) &= \mathbb{E}_{x \sim \mathcal{D}, \{y_k\} \sim \pi_{\theta_{\text{old}}}(\cdot|x)} \left[ \frac{1}{K} \sum_{k=1}^K \frac{1}{T_k} \sum_{t=1}^{T_k} \right. \\ &\quad \left. g_{k,t}(\theta, x) - \beta_{\text{KL}} \mu_{\text{KL}}(\pi_{\theta} \parallel \pi_{\text{ref}}) \right], \\ \text{s.t. } g_{k,t}(\theta, x) &= \min \left( \rho_{k,t}(\theta) A_{k,t}(x), \tilde{\rho}_{k,t}(\theta) A_{k,t}(x) \right), \end{aligned} \quad (8)$$

where  $\beta_{\text{KL}}$ ,  $\rho_{k,t}(\theta)$ , and  $\tilde{\rho}_{k,t}(\theta)$  are the same as in Eq.2. Based on this,  $GC^2PO$  drives the LLMs to generate episodes that are both outcome-successful and counterfactually robust, learning generalizable reasoning patterns.

## 4. Experiments

In this section, we conduct extensive experiments on various reasoning benchmarks to evaluate the effectiveness of  $GC^2PO$ . See Appendix E-G for more details and results.

### 4.1. Experimental Settings

We evaluate on a range of reasoning benchmarks, including AIME24-25, AMC, MATH500 (Hendrycks et al., 2021), MinervaMATH (Lewkowycz et al., 2022), GSM8K (Cobbe et al., 2021), and HumanEval (Chen et al., 2021), and base models with different scales, e.g., 1.5B of DeepScaleR-1.5B-Preview and DeepSeek-R1-Distill-Qwen-1.5B, 7B of Qwen2.5-7B-Instruct and DeepSeek-R1-Distill-Qwen-7B, etc. We compare  $GC^2PO$  against (i) outcome-reward RL methods, e.g., GRPO (Shao et al., 2024), Dr.GRPO (Liu et al., 2025), etc., and (ii) process-reward RL methods, e.g., GCPO (Gu et al., 2025), MRT (Qu et al., 2025), L2T-GRPO (Wang et al., 2025b), etc. Following (Qu et al., 2025; Wang et al., 2025b), DeepScaleR-1.5B-Preview, which has already been fine-tuned on 40k math QA pairs, is further fine-tuned on 919 AIME problems. DeepSeek-R1-Distill-Qwen-1.5B and 7B are fine-tuned on a random subset of 4,000 NuminaMath QA pairs (Li et al., 2024). For optimization, we use a learning rate of  $1 \times 10^{-6}$ , weight decay of 0.01, and batch size 256. The hyperparameters  $\lambda_{\text{exp}}$  and  $\lambda_{\text{cf}}$  are set to 0.9 and 0.8, respectively. All experiments are conducted on A100 GPU clusters. See Appendix F for more details.

### 4.2. Results

**Performance and Generalization Analyses.** We evaluate  $GC^2PO$  across all the benchmarks and base models, measuring both pass@1 accuracy and total token usage. As shown in Table 1 and Appendix G.2, (i)  $GC^2PO$  achieves the best performance, attaining the best reasoning accuracy with relatively fewer tokens, e.g.,  $GC^2PO$  improves pass@1 by over 2.5% against the baselines; (ii)  $GC^2PO$  consistently outperforms baselines on datasets whose distributions differ from the training data, demonstrating great generalization.

**Trade-off Performance.** To compare efficiency, we (i) normalize the computational cost of GRPO to  $1 \times$  and report all methods' results, measuring total GPU hours under matched schedules and hardware; and (ii) sample reasoning trajectories with a fixed token context window and truncate them at different budgets to evaluate performance. Figure 4 show that  $GC^2PO$  incurs only a modest overhead of  $1.2 \times$ , while achieving the best reasoning accuracy with lower budget.

**Training Stability.** Since the training of LLMs is costly, stable optimization is essential to ensure efficient convergence and avoid wasted compute. Following common practice in RL-based training, we use the gradient norm as a proxy for policy variance. Besides, we record the sampling ratio of our method compared to previous sequence-level methods. As shown in Figure 5,  $GC^2PO$  exhibits more stable training, with its gradient norm remaining nearly constant throughout training and the sampling ratio achieving no obvious spikes.

**Visualization Analysis.** To illustrate how  $GC^2PO$  changes model behavior, we qualitatively compare models fine-tuned by different methods, visualizing their reasoning traces. Figure 6 and Appendix G.5 show that  $GC^2PO$  yields more structured reasoning: it decomposes problems into clear subgoals, revisits intermediate steps, and corrects inconsistencies; while GRPO often commits to a single rigid line of reasoning, even when the underlying reasoning is flawed.

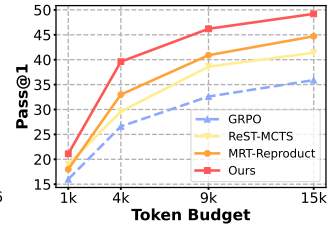
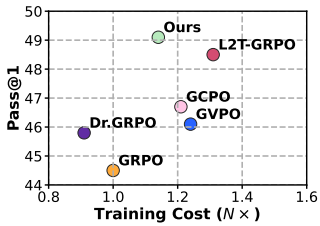
**Ablation Study.** We conduct experiments on the hyperparameters  $\lambda_{\text{exp}}$  and  $\lambda_{\text{cf}}$ . We search  $\lambda_{\text{exp}}$  and  $\lambda_{\text{cf}}$  over  $[0, 1]$ . Note that when they equal 0, we examine two ablated variants: (i)  $GC^2PO$  w/o  $S_{\text{exp}}$ ; (ii)  $GC^2PO$  w/o  $S_{\text{neq}}$ ; (iii)  $GC^2PO$  w/o  $S_{\text{sta}} \& S_{\text{exp}}$  (also two terms of  $R_{\text{cf}}^*$ ). Figure 7 (i) demonstrates the effectiveness of each component within  $GC^2PO$ . (ii) shows that the optimal result is at  $\lambda_{\text{exp}} = 0.9$  and  $\lambda_{\text{cf}} = 0.8$ , which are our final configuration.

## 5. Related Work

Complex reasoning remains a challenging capability for LLMs (Jimenez et al., 2024; Snell et al., 2024). To improve reasoning performance, several works (Snell et al., 2024; Wang et al., 2025a;d; Ye et al., 2025b) adopt RL-based post-training methods, which has become a key component of LLM post-training. Among these methods, GRPO (Shao et al., 2024) and its variants (Zhao et al., 2025; Gu et al., 2025; Liu et al., 2025) have attracted particular interest, as they simplify optimization by using the group's average reward as an advantage baseline, making them well-suited for fine-tuning large-scale models. However, they rely on binary rewards that reflect only outcome correctness, ignoring the reasoning process (Wang et al., 2025b; Zheng et al., 2025a). To address this, some works introduce process rewards to evaluate intermediate steps (Qu et al., 2025; Zeng et al., 2025; Zheng et al., 2025b; Zeng et al., 2025; Wang et al.,

Table 1. Pass@1 performance on various reasoning benchmarks. We compare base models trained with different approaches. The best results are highlighted in **bold**. “(+)” denotes the improvement over models without fine-tuning. More results are provided in Appendix G.

Methods	AIME 2024	AIME 2025	AMC 2023	MATH500	MinervaMATH	GSM8K	Average Results
<b>DeepScaleR-1.5B-Preview</b>	42.8	36.7	83.0	85.2	24.6	89.6	60.3
+ GRPO (Shao et al., 2024)	44.5 (+1.7)	39.3 (+2.6)	81.5 (-1.5)	84.9 (-0.3)	24.7 (+0.1)	89.4 (-0.2)	60.7 (+0.4)
+ length penalty (Arora & Zanette, 2025)	40.3 (-2.5)	30.3 (-6.4)	77.3 (-5.7)	83.2 (-2.0)	23.0 (-1.6)	88.5 (-1.1)	57.1 (-3.2)
+ ReST-MCTS (Zhang et al., 2024)	45.5 (+2.7)	39.5 (+2.8)	83.4 (+0.4)	84.8 (-0.4)	23.9 (-0.7)	89.9 (+0.3)	61.2 (+0.9)
+ GVPO (Zhang et al., 2025a)	46.1 (+3.3)	39.7 (+3.0)	83.6 (+0.6)	85.7 (+0.5)	25.3 (+0.7)	90.4 (+0.8)	61.8 (+1.5)
+ Dr.GRPO (Liu et al., 2025)	45.8 (+3.0)	39.6 (+2.9)	82.1 (-0.9)	85.3 (+0.1)	25.1 (+0.5)	90.0 (+0.4)	61.3 (+1.0)
+ GCPO (Gu et al., 2025)	46.7 (+3.9)	40.3 (+3.6)	84.1 (+1.1)	86.3 (+1.1)	25.9 (+1.4)	90.5 (+0.9)	62.3 (+2.0)
+ MRT (Qu et al., 2025)	47.2 (+4.4)	39.7 (+3.0)	83.1 (+0.1)	85.1 (-0.1)	24.2 (-0.4)	89.9 (+0.3)	61.5 (+1.2)
+ L2T-GRPO (Wang et al., 2025b)	48.5 (+5.7)	40.2 (+3.5)	85.4 (+2.4)	88.1 (+2.9)	26.5 (+1.9)	90.9 (+1.3)	63.3 (+3.0)
+ GC <sup>2</sup> PO (Ours)	<b>49.3 (+6.2)</b>	<b>40.6 (+3.9)</b>	<b>86.1 (+3.1)</b>	<b>88.3 (+3.1)</b>	<b>27.5 (+2.9)</b>	<b>91.6 (+2.0)</b>	<b>63.9 (+3.6)</b>
<b>DeepSeek-R1-Distill-Qwen-1.5B</b>	28.7	26.0	69.9	80.1	19.8	83.4	51.3
+ GRPO (Shao et al., 2024)	29.8 (+1.1)	27.3 (+1.3)	70.5 (+0.6)	80.3 (+0.2)	22.1 (+2.3)	84.5 (+1.1)	52.4 (+1.1)
+ length penalty (Arora & Zanette, 2025)	27.5 (-1.2)	22.6 (-3.4)	64.4 (-5.5)	77.1 (-3.0)	18.8 (-1.0)	82.6 (-0.8)	48.8 (-2.5)
+ ReST-MCTS (Zhang et al., 2024)	30.5 (+1.8)	28.6 (+2.6)	71.1 (+1.2)	80.4 (+0.3)	20.3 (+0.5)	84.8 (+1.4)	52.6 (+1.3)
+ GVPO (Zhang et al., 2025a)	30.6 (+1.9)	28.2 (+2.2)	71.5 (+1.6)	80.5 (+0.4)	23.1 (+3.3)	85.0 (+1.6)	53.2 (+1.8)
+ Dr.GRPO (Liu et al., 2025)	30.4 (+1.7)	28.4 (+2.4)	71.3 (+1.4)	80.8 (+0.7)	22.9 (+3.1)	85.0 (+1.6)	53.1 (+1.8)
+ GCPO (Gu et al., 2025)	31.0 (+2.3)	29.0 (+3.0)	71.8 (+1.9)	81.6 (+1.5)	23.4 (+3.6)	85.3 (+1.9)	53.7 (+2.4)
+ MRT (Qu et al., 2025)	30.3 (+1.6)	29.3 (+3.3)	72.9 (+3.0)	80.4 (+0.3)	22.5 (+2.7)	84.7 (+1.3)	53.4 (+2.0)
+ L2T-GRPO (Wang et al., 2025b)	32.9 (+4.2)	30.1 (+4.1)	73.5 (+3.6)	84.7 (+4.6)	24.5 (+4.7)	85.5 (+2.1)	55.2 (+3.9)
+ GC <sup>2</sup> PO (Ours)	<b>33.8 (+5.1)</b>	<b>30.7 (+4.7)</b>	<b>74.3 (+4.4)</b>	<b>85.3 (+5.2)</b>	<b>25.4 (+5.7)</b>	<b>86.5 (+3.1)</b>	<b>55.9 (+4.6)</b>
<b>DeepSeek-R1-Distill-Qwen-7B</b>	55.5	50.2	85.1	87.4	42.1	91.6	68.6
+ GRPO (Shao et al., 2024)	56.9 (+1.4)	51.7 (+1.5)	85.5 (+0.4)	87.7 (+0.3)	43.5 (+1.4)	92.1 (+0.5)	69.6 (+0.9)
+ length penalty (Arora & Zanette, 2025)	53.8 (-1.7)	46.9 (-3.3)	81.2 (-3.9)	83.7 (-3.7)	39.5 (-2.6)	91.1 (-0.5)	66.0 (-2.6)
+ ReST-MCTS (Zhang et al., 2024)	57.1 (+1.6)	52.4 (+2.2)	85.7 (+0.6)	87.9 (+0.5)	42.8 (+0.7)	92.0 (+0.4)	69.7 (+1.0)
+ GVPO (Zhang et al., 2025a)	57.5 (+2.0)	52.1 (+1.9)	86.3 (+1.2)	88.5 (+1.1)	44.2 (+2.1)	92.9 (+1.3)	70.3 (+1.6)
+ Dr.GRPO (Liu et al., 2025)	57.4 (+1.9)	52.3 (+2.1)	86.4 (+1.3)	88.2 (+0.8)	44.0 (+1.9)	92.3 (+0.7)	70.1 (+1.5)
+ GCPO (Gu et al., 2025)	58.3 (+2.8)	53.0 (+2.8)	87.3 (+2.2)	89.1 (+1.7)	45.0 (+2.9)	92.6 (+1.0)	70.9 (+2.2)
+ MRT (Qu et al., 2025)	57.0 (+1.5)	52.4 (+2.2)	86.0 (+0.9)	88.4 (+1.0)	44.3 (+2.2)	92.2 (+0.6)	70.1 (+1.4)
+ L2T-GRPO (Wang et al., 2025b)	58.4 (+2.9)	53.6 (+3.4)	87.5 (+2.4)	89.2 (+1.8)	45.0 (+2.9)	92.9 (+1.3)	71.1 (+2.5)
+ GC <sup>2</sup> PO (Ours)	<b>59.1 (+3.6)</b>	<b>54.3 (+4.1)</b>	<b>88.2 (+3.1)</b>	<b>89.8 (+2.4)</b>	<b>45.6 (+3.5)</b>	<b>93.6 (+2.0)</b>	<b>71.8 (+3.1)</b>



(a) Training time vs. Pass@1. (b) Token budget vs. Pass@1.

Figure 4. Trade-off performance of different methods.

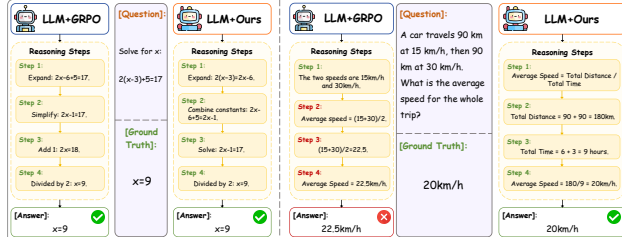
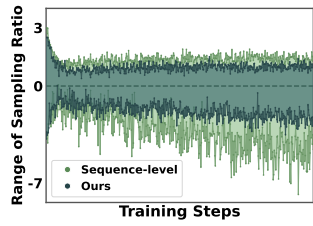
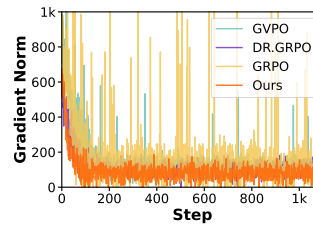


Figure 6. Qualitative Results (See Appendix G.5.1 for full results).

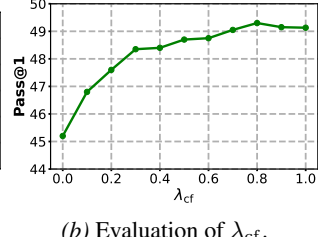
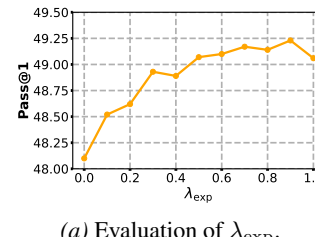
2025b), but still primarily target final correctness and may undermine the reasoning reliability, affecting generalization. To address this, we propose an episodic causal counterfactual reward for policy optimization that explicitly decouples the reasoning quality from answer correctness, encouraging LLMs to acquire generalizable reasoning strategies. See Appendix D for more comparisons and discussions.



(a) Gradient norm.

(b) Sampling ratio.

Figure 5. Evaluation of training stability.



(a) Evaluation of  $\lambda_{\text{exp}}$ . (b) Evaluation of  $\lambda_{\text{cf}}$ .

Figure 7. Ablation Studies (See Appendix G.4 for full results).

## 6. Conclusion

In this paper, we explore a critical bottleneck in GRPO-based post-training: the reward mechanisms of existing methods entangle process validity with final correctness, hindering the acquisition of generalizable reasoning. To overcome this, we establish a causal perspective that formalizes multi-candidate generation as a set of counterfactual ex-

periments and propose Group Causal Counterfactual Policy Optimization (GC<sup>2</sup>PO). It introduces a fine-grained reward mechanism to jointly evaluate the robustness and effectiveness of reasoning episodes under mechanism-preserving perturbations. This design decouples reasoning quality from outcome luck: it provides positive supervision for logically sound reasoning steps, while suppressing spurious shortcuts and lucky guesses. By combining it with outcome reward, we build token-level advantage for optimization, encouraging LLMs to favor reasoning patterns that are both process-valid and answer-correct. Extensive experiments across diverse benchmarks demonstrate its advantages.

## Impact Statement

This paper presents work whose goal is to advance the field of machine learning. There are many potential societal consequences of our work, none of which we feel must be specifically highlighted here.

## References

Arora, D. and Zanette, A. Training language models to reason efficiently. *arXiv preprint arXiv:2502.04463*, 2025.

Avron, H. A generalized courant-fischer minimax theorem. 2008.

Cazenave, T. and Haraux, A. *An introduction to semilinear evolution equations*, volume 13. Oxford University Press, 1998.

Chen, M., Tworek, J., Jun, H., Yuan, Q., Pinto, H. P. D. O., Kaplan, J., Edwards, H., Burda, Y., Joseph, N., Brockman, G., et al. Evaluating large language models trained on code. *arXiv preprint arXiv:2107.03374*, 2021.

Chen, Z., Qin, X., Wu, Y., Ling, Y., Ye, Q., Zhao, W. X., and Shi, G. Pass@ k training for adaptively balancing exploration and exploitation of large reasoning models. *arXiv preprint arXiv:2508.10751*, 2025.

Cobbe, K., Kosaraju, V., Bavarian, M., Chen, M., Jun, H., Kaiser, L., Plappert, M., Tworek, J., Hilton, J., Nakano, R., et al. Training verifiers to solve math word problems. *arXiv preprint arXiv:2110.14168*, 2021.

Dontchev, A. and Hager, W. An inverse mapping theorem for set-valued maps. *Proceedings of the American Mathematical Society*, 121(2):481–489, 1994.

Gu, Z., Wang, J., Zuo, R., Sun, C., Song, Z., Zheng, C., and Qiang, W. Group causal policy optimization for post-training large language models. *arXiv preprint arXiv:2508.05428*, 2025.

Hendrycks, D., Burns, C., Kadavath, S., Arora, A., Basart, S., Tang, E., Song, D., and Steinhardt, J. Measuring mathematical problem solving with the math dataset. *arXiv preprint arXiv:2103.03874*, 2021.

Jimenez, C. E., Yang, J., Wettig, A., Yao, S., Pei, K., Press, O., and Narasimhan, K. Swe-bench: Can language models resolve real-world github issues?, 2024. URL <https://arxiv.org/abs/2310.06770>.

Khalifa, M., Agarwal, R., Logeswaran, L., Kim, J., Peng, H., Lee, M., Lee, H., and Wang, L. Process reward models that think. *arXiv preprint arXiv:2504.16828*, 2025.

Lewkowycz, A., Andreassen, A., Dohan, D., Dyer, E., Michalewski, H., Ramasesh, V., Sloane, A., Anil, C., Schlag, I., Gutman-Solo, T., et al. Solving quantitative reasoning problems with language models. *Advances in Neural Information Processing Systems*, 35:3843–3857, 2022.

Li, J., Beeching, E., Tunstall, L., Lipkin, B., Soletskyi, R., Huang, S., Rasul, K., Yu, L., Jiang, A. Q., Shen, Z., et al. Numinamath: The largest public dataset in ai4maths with 860k pairs of competition math problems and solutions. *Hugging Face repository*, 13:9, 2024.

Liu, Z., Chen, C., Li, W., Qi, P., Pang, T., Du, C., Lee, W. S., and Lin, M. Understanding r1-zero-like training: A critical perspective. *arXiv preprint arXiv:2503.20783*, 2025.

Ness, R., Paneri, K., and Vitek, O. Integrating markov processes with structural causal modeling enables counterfactual inference in complex systems. *Advances in Neural Information Processing Systems*, 32, 2019.

Oberst, M. and Sontag, D. Counterfactual off-policy evaluation with gumbel-max structural causal models. In *International Conference on Machine Learning*, pp. 4881–4890. PMLR, 2019.

Pazy, A. *Semigroups of linear operators and applications to partial differential equations*, volume 44. Springer Science & Business Media, 2012.

Pearl, J. *Causality*. Cambridge university press, 2009.

Qu, Y., Yang, M. Y., Setlur, A., Tunstall, L., Beeching, E. E., Salakhutdinov, R., and Kumar, A. Optimizing test-time compute via meta reinforcement fine-tuning. *arXiv preprint arXiv:2503.07572*, 2025.

Sadik, A. R. and Govind, S. Benchmarking llm for code smells detection: Openai gpt-4.0 vs deepseek-v3, 2025. URL <https://arxiv.org/abs/2504.16027>.

Shao, Z., Wang, P., Zhu, Q., Xu, R., Song, J., Bi, X., Zhang, H., Zhang, M., Li, Y. K., Wu, Y., and Guo, D. Deepseekmath: Pushing the limits of mathematical reasoning in open language models, 2024. URL <https://arxiv.org/abs/2402.03300>.

Snell, C., Lee, J., Xu, K., and Kumar, A. Scaling llm test-time compute optimally can be more effective than scaling model parameters, 2024. URL <https://arxiv.org/abs/2408.03314>.

Szepesvári, C. *Algorithms for reinforcement learning*. Springer nature, 2022.

Tan, H., Pan, J., Lin, J., Chen, T., Zheng, Z., Tang, Z., and Yang, H. Gtpo and grp-s: Token and sequence-level reward shaping with policy entropy. *arXiv preprint arXiv:2508.04349*, 2025.

Tie, G., Zhao, Z., Song, D., Wei, F., Zhou, R., Dai, Y., Yin, W., Yang, Z., Yan, J., Su, Y., et al. A survey on post-training of large language models. *arXiv e-prints*, pp. arXiv–2503, 2025.

Wang, C., Zhao, Z., Jiang, Y., Chen, Z., Zhu, C., Chen, Y., Liu, J., Zhang, L., Fan, X., Ma, H., et al. Beyond reward hacking: Causal rewards for large language model alignment. *arXiv preprint arXiv:2501.09620*, 2025a.

Wang, J., Qiang, W., Song, Z., Zheng, C., and Xiong, H. Learning to think: Information-theoretic reinforcement fine-tuning for llms. *arXiv preprint arXiv:2505.10425*, 2025b.

Wang, N., Yao, B., Zhou, J., Hu, Y., Wang, X., Guan, N., and Jiang, Z. Insights from verification: Training a verilog generation llm with reinforcement learning with testbench feedback, 2025c. URL <https://arxiv.org/abs/2504.15804>.

Wang, Y., Liu, Q., Xu, J., Liang, T., Chen, X., He, Z., Song, L., Yu, D., Li, J., Zhang, Z., Wang, R., Tu, Z., Mi, H., and Yu, D. Thoughts are all over the place: On the underthinking of o1-like llms, 2025d. URL <https://arxiv.org/abs/2501.18585>.

Wang, Z., Zhang, J., Zhao, W., Farnia, F., and Yu, B. Moreaupruner: Robust pruning of large language models against weight perturbations. *arXiv preprint arXiv:2406.07017*, 2024.

Wiering, M. A. and Van Otterlo, M. Reinforcement learning. *Adaptation, learning, and optimization*, 12(3):729, 2012.

Yang, J., Lin, K., and Yu, X. Think when you need: Self-adaptive chain-of-thought learning, 2025. URL <https://arxiv.org/abs/2504.03234>.

Ye, C., Yu, Z., Zhang, Z., Chen, H., Sadagopan, N., Huang, J., Zhang, T., and Beniwal, A. Beyond correctness: Harmonizing process and outcome rewards through rl training. *arXiv preprint arXiv:2509.03403*, 2025a.

Ye, G., Pham, K. D., Zhang, X., Gopi, S., Peng, B., Li, B., Kulkarni, J., and Inan, H. A. On the emergence of thinking in llms i: Searching for the right intuition. *arXiv preprint arXiv:2502.06773*, 2025b.

Yeo, E., Tong, Y., Niu, M., Neubig, G., and Yue, X. Demystifying long chain-of-thought reasoning in llms, 2025. URL <https://arxiv.org/abs/2502.03373>.

Zeng, T., Zhang, S., Wu, S., Classen, C., Chae, D., Ewer, E., Lee, M., Kim, H., Kang, W., Kunde, J., et al. Versaprm: Multi-domain process reward model via synthetic reasoning data. *arXiv preprint arXiv:2502.06737*, 2025.

Zhang, D., Zhoubian, S., Hu, Z., Yue, Y., Dong, Y., and Tang, J. Rest-mcts\*: Llm self-training via process reward guided tree search. *Advances in Neural Information Processing Systems*, 37:64735–64772, 2024.

Zhang, K., Hong, Y., Bao, J., Jiang, H., Song, Y., Hong, D., and Xiong, H. Gypo: Group variance policy optimization for large language model post-training. *arXiv preprint arXiv:2504.19599*, 2025a.

Zhang, Z., Zheng, C., Wu, Y., Zhang, B., Lin, R., Yu, B., Liu, D., Zhou, J., and Lin, J. The lessons of developing process reward models in mathematical reasoning. *arXiv preprint arXiv:2501.07301*, 2025b.

Zhao, Y., Liu, Y., Liu, J., Chen, J., Wu, X., Hao, Y., Lv, T., Huang, S., Cui, L., Ye, Q., et al. Geometric-mean policy optimization. *arXiv preprint arXiv:2507.20673*, 2025.

Zheng, C., Liu, S., Li, M., Chen, X.-H., Yu, B., Gao, C., Dang, K., Liu, Y., Men, R., Yang, A., et al. Group sequence policy optimization. *arXiv preprint arXiv:2507.18071*, 2025a.

Zheng, C., Zhu, J., Lin, J., Dai, X., Yu, Y., Zhang, W., and Yang, M. Cold: Counterfactually-guided length debiasing for process reward models. *arXiv preprint arXiv:2507.15698*, 2025b.

Zhou, Y., Jiang, S., Tian, Y., Weston, J., Levine, S., Sukhbaatar, S., and Li, X. Sweet-rl: Training multi-turn llm agents on collaborative reasoning tasks, 2025. URL <https://arxiv.org/abs/2503.15478>.

Zimmermann, R. S., Sharma, Y., Schneider, S., Bethge, M., and Brendel, W. Contrastive learning inverts the data generating process. In *International conference on machine learning*, pp. 12979–12990. PMLR, 2021.